geoconvention
Calgary • Canada • May 11-13 2026

Induced-Seismicity-Driven Geological Modeling of the Steep Creek Reef Incorporating the Gold Creek Seismic Cluster

Jinze Xu[1], Tyler Hauck[1], Mauricio Reyes Canales[1], Claudio Virues[2], Baohong Yang[1], Chet Goerzen[1], Alexandra Robertson[2], Shaurat Sayani[1], Nick Roman[1]*

[1]Alberta Geological Survey, Alberta Energy Regulator

[2]Regulatory Applications, Alberta Energy Regulator

** Corresponding Author: Mauricio.Canales@aer.ca*

Summary

Recent instances of disposal-related induced seismicity have led to the production of a 3D geological model of the Leduc Formation Steep Creek reef in west-central Alberta. Unlike traditional modeling approaches, the design of this model was guided by seismic activity, specifically incorporating the Gold Creek seismic cluster, to better capture the subsurface dynamics associated with induced events. The geological framework incorporates formation tops, while property modeling establishes porosity-permeability relationships from core data. Seismic events within the Gold Creek seismic cluster were used to define a polygon that divides the model into induced seismicity and non-induced seismicity sectors, enabling focused analysis within the Gold Creek seismic cluster. Pressure modeling based on reservoir pressure measurements shows pressure buildup in the induced seismicity sector tracking injection rate increases during the study period. The simulation-ready model applies to local grid refinement in the induced seismicity sector while using coarser cells in the non-induced seismicity sector. This induced-seismicity-driven workflow integrates geology and geophysics, providing a simulation-ready framework for analyzing temporal relationships between injection activities, pressure evolution, and induced seismicity related to water disposal activities.

Introduction

The Leduc Formation Steep Creek reef is located approximately 9 km west of the Leduc Gold Creek reef complex (Fig. 1). This Late Devonian Leduc reef buildup is considerably larger than Gold Creek[1,2]. Nine water disposal injectors currently operate within the Leduc Formation at Steep Creek (Fig. 2), with injection starting in June 2015.

Recent work has linked the Gold Creek seismic cluster to water disposal into the Leduc Steep Creek buildup[1]. This thick carbonate reef has seen injection rates climb steadily over time. From August 2019 through October 2025, more than 550 earthquakes (M_1 = 1.00 to 4.50) occurred in the Gold Creek sequence [4]. Eight of these exceeded M>3.0, including the largest at M=4.50 in October 2024.

A need to better understand the spatiotemporal context of these observations drove the desire for an integrated geological model of Steep Creek that incorporates the seismicity associated with the Gold Creek cluster. Our approach has started with a preliminary 3D geological model that links geology and seismology to understand how seismic events distribute within geological structures, track pressure changes, and create a solid foundation for reservoir simulation.

We used publicly available data from AccuMap[3] and the Alberta Geological Survey Earthquake Dashboard[4]. Our workflow has five main components: (1) modeling of the Leduc Formation, (2)

property modeling for porosity and permeability, (3) induced-seismicity-driven geometrical modeling to define induced seismicity sectors, (4) induced-seismicity-driven pressure analysis using reservoir pressure measurements within the induced seismicity sector, and (5) induced-seismicity-driven simulation model upscaling with local grid refinement.

Pore pressure evolution is a key mechanism in induced seismicity by reducing effective stress on critically stressed faults and triggering their reactivation [5,6]. Given the limited seismic reflection data and challenges in mapping faults precisely, this study focuses on characterizing pressure dynamics—a common approach when detailed fault geometry is unavailable [6]. The analysis acknowledges the broader suite of coupled hydro-mechanical processes including poroelastic effects and fault reactivation [7-10].

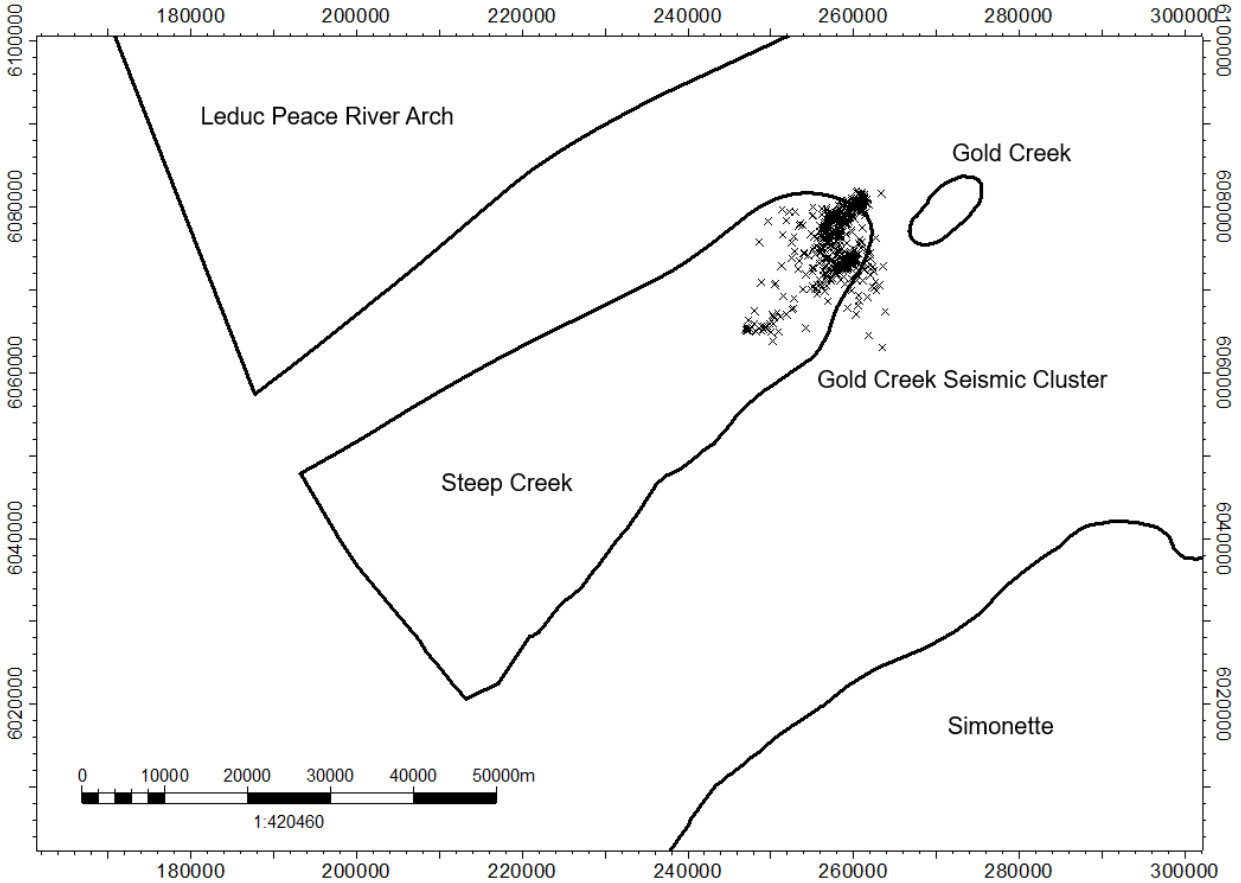


Figure 1. Location of the Leduc Formation Steep Creek buildup and the associated Gold Creek seismic cluster

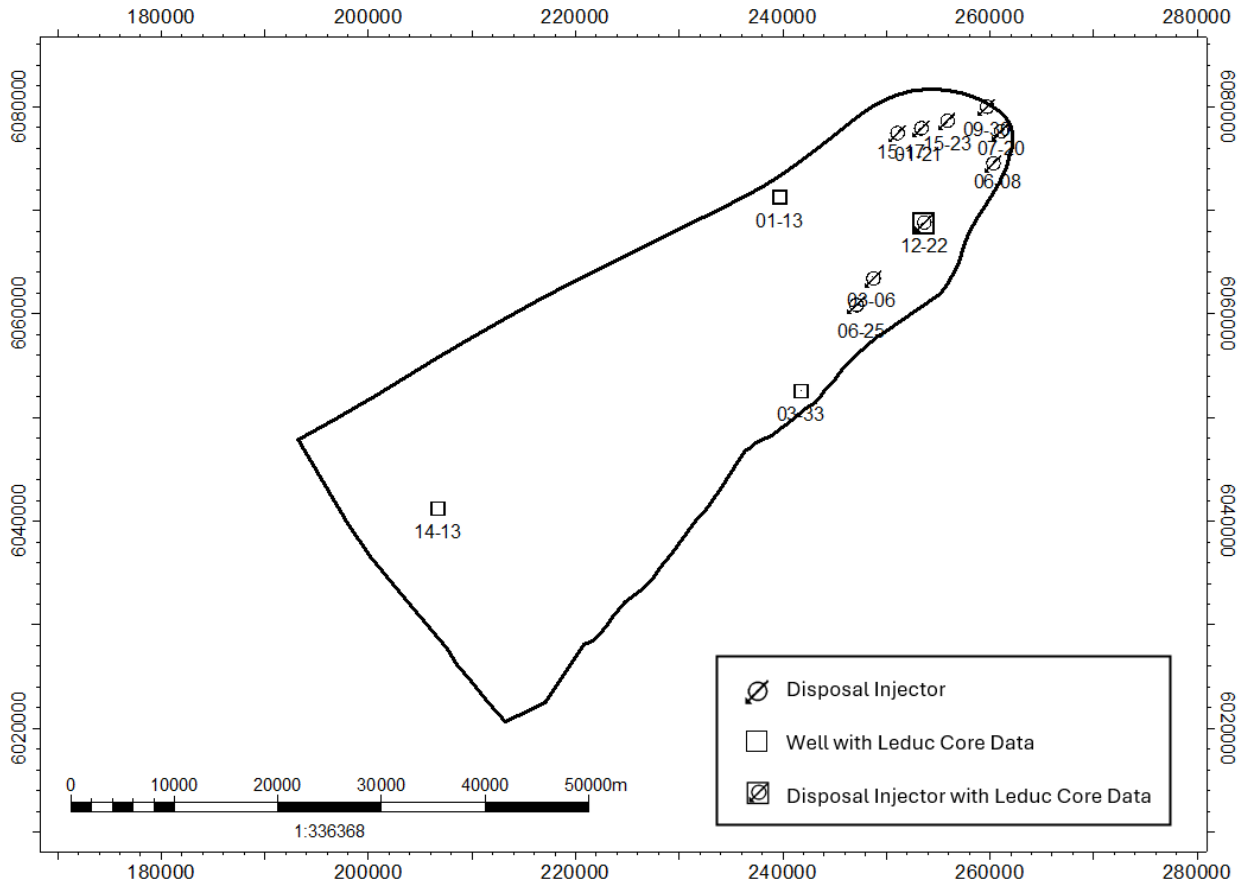


Figure 2. Water disposal wells and wells with Leduc Formation core data from the Steep Creek buildup.

3D Modeling Framework

The geological framework was built using formation tops from 218 wells for the base and top of the Leduc Formation (Figure 3). The resulting model has 100 m × 100 m horizontal cells and 2 m vertical resolution (Fig. 4). As the study is in a preliminary stage, subdivision of the Leduc Formation into finer resolution depositional sequences was not attempted. Grid quality was checked by confirming zero cell inversions and positive cell volumes throughout [11].

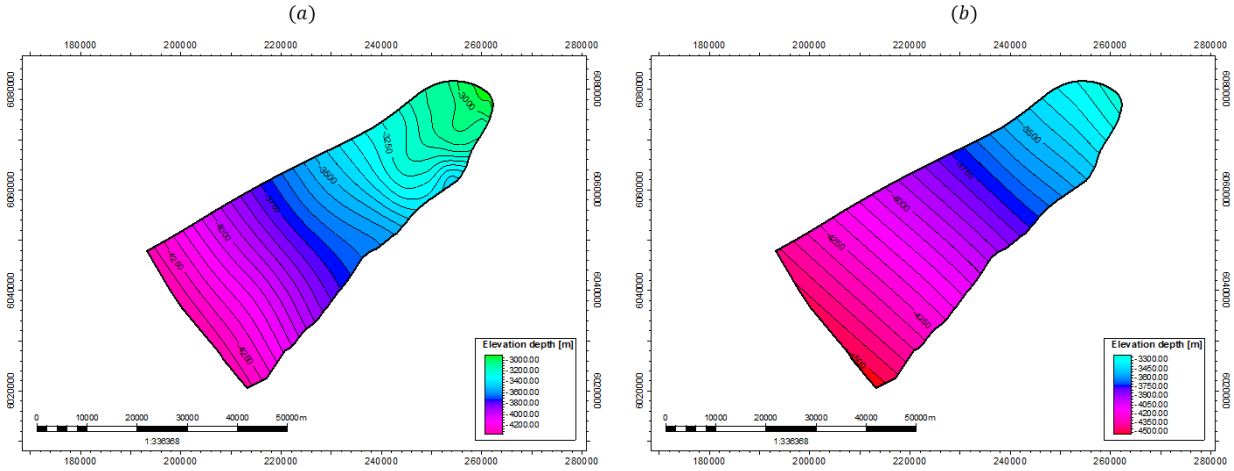


Figure 3. (a) Structure top of Leduc Formation. (b) Structural base surface of Leduc formation.

Property Modeling

Property modeling defines porosity, horizontal permeability, vertical permeability, and saturation distributions. The Leduc Formation at Steep Creek is fully water saturated, so water saturation equals 1.0 across the model. For porosity and permeability, we used core data from four wells (Fig. 2): one disposal injector and three offset wells within about 1,000 m of injection operations. Limited data prevented geostatistical interpolation or separate modeling of matrix, fractures, and vugs, so we used a homogeneous single-porosity approach at this initial stage of the project. It is realized that some lateral and vertical heterogeneity is almost certainly present, based on Devonian facies models and other buildups in the basin, and will be further investigated at a later stage in the project. Both coring locations and perforation zones fall within the upper 200 m below the Leduc top, confirming that the established petrophysical relationships are applicable to and representative of the active disposal interval.

Raw porosity-permeability data show considerable scatter (Fig. 4a, 5a). Permeability values were grouped by 0.01 porosity bins, and geometric means were calculated for each bin (Fig. 4b, 5b)[12]. Cross-plots of these upscaled values show exponential increase in permeability with porosity (Fig. 4c, 5c), and is attributed to the dolomitization of the buildup (cf. Amthor et al. 1994) [12].

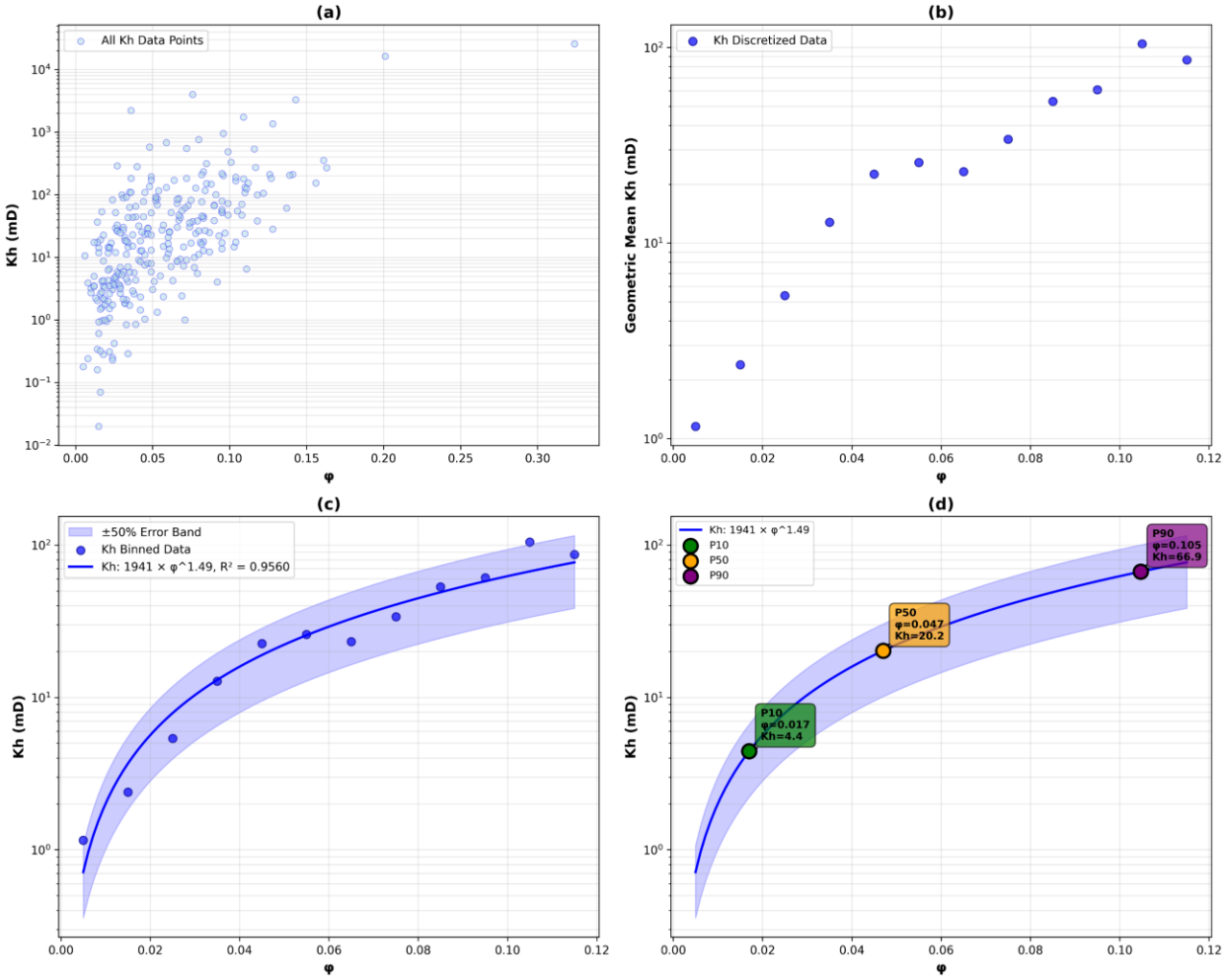


Figure 4. (a) Raw data of horizontal permeability and porosity. (b) Upscaling of horizontal permeability based on 0.01 porosity bin. (c) Correlation between horizontal permeability and porosity after upscaling. (d) P10, P50 and P90 porosity and horizontal permeability.

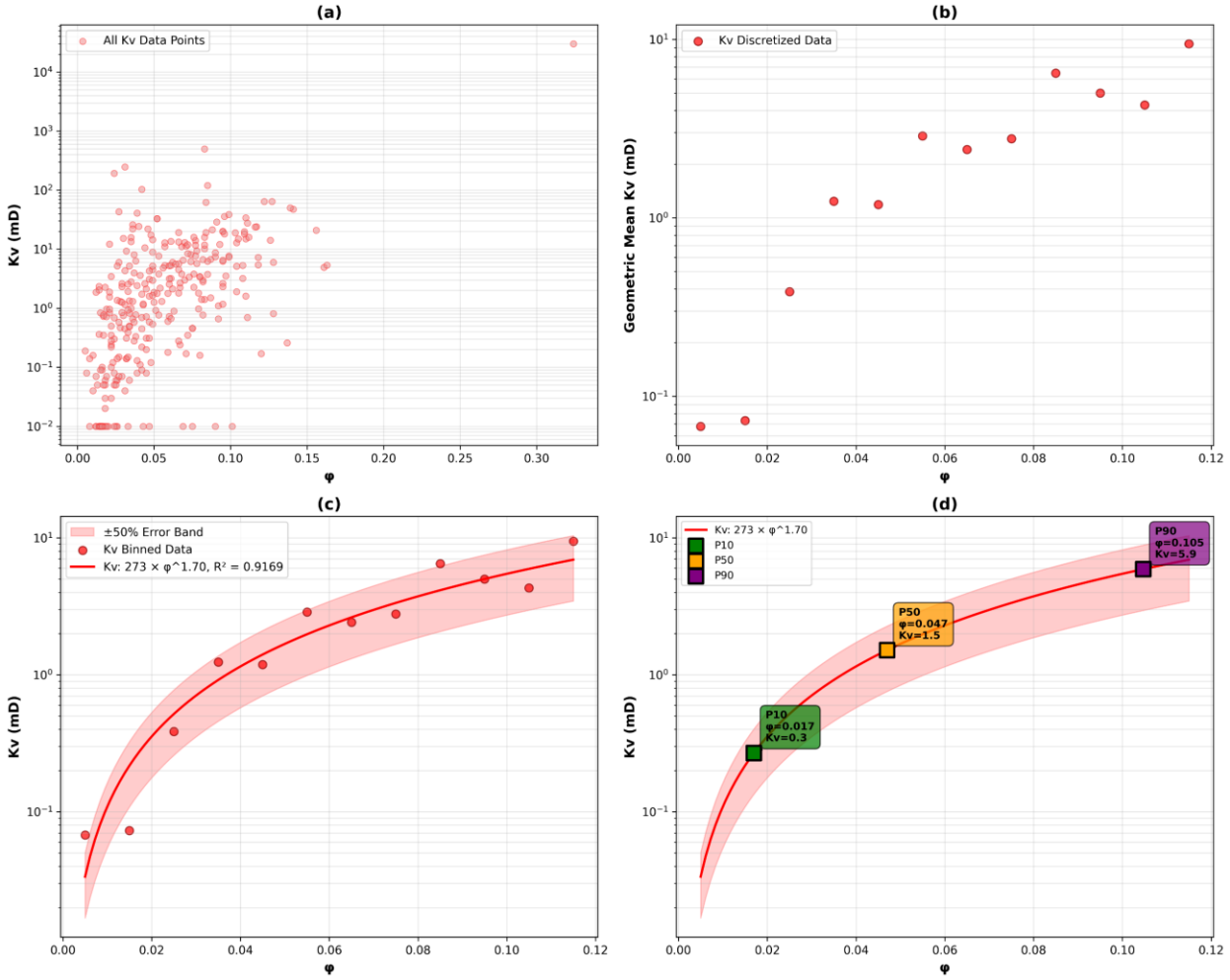


Figure 5. (a) Raw data of vertical permeability and porosity. (b) Upscaling of vertical permeability based on 0.01 porosity bin. (c) Correlation between vertical permeability and porosity after upscaling. (d) P10, P50 and P90 porosity and vertical permeability.

The base property model (Fig. 6) uses P50 values: 4.7% porosity, 20.2 mD horizontal permeability (Kh), and 1.5 mD vertical permeability (Kv) from the porosity-permeability correlation. P10 and P90 values are collected (Fig. 4d, 5d) for future uncertainty work during reservoir simulation stages.

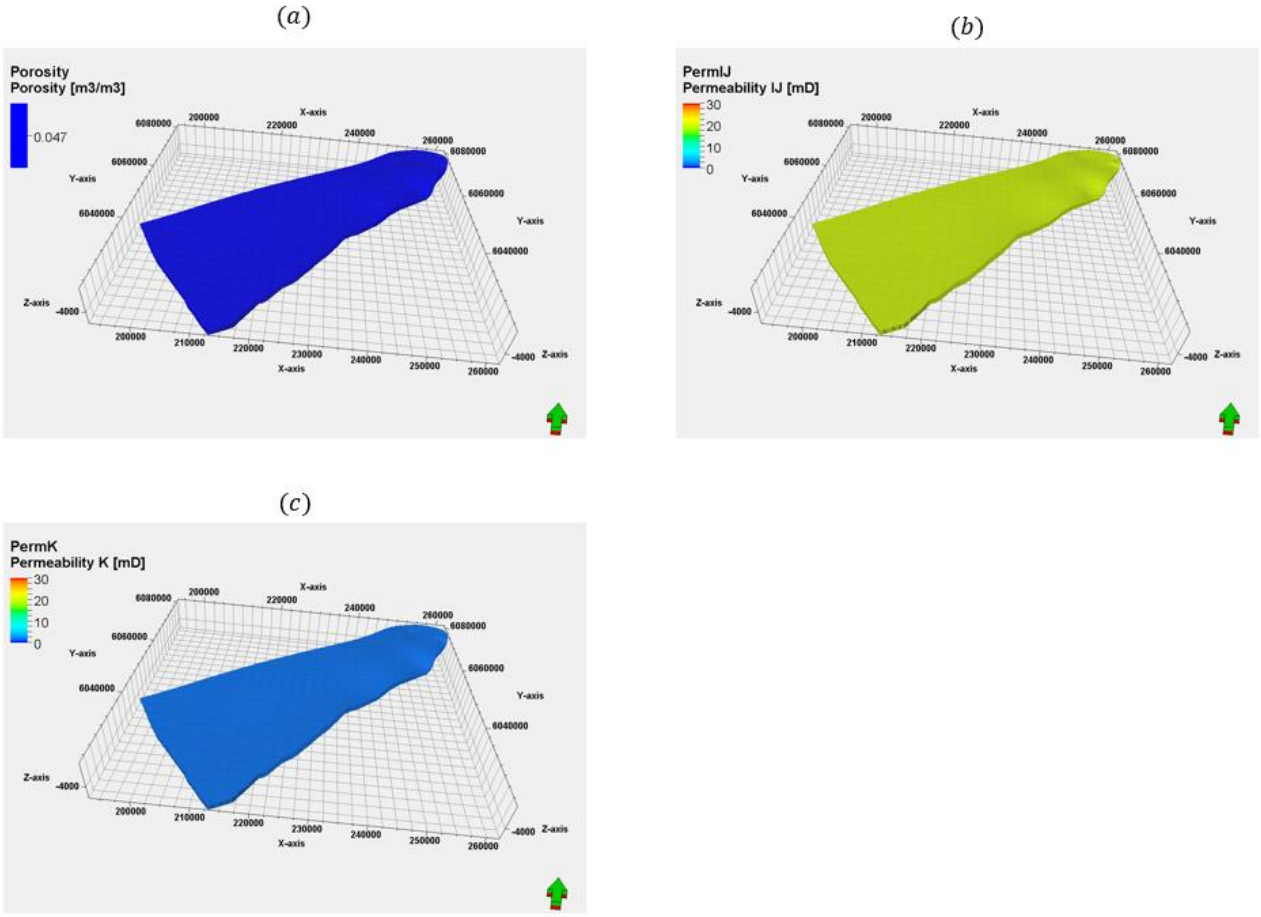


Figure 6. (a) Property model: P50 porosity. (b) Property model: P50 horizontal permeability. (c) Property model: P50 vertical permeability.

Induced-Seismicity-Driven Geometrical Modeling

Incorporating the 569 seismic events into the model was critical for targeted pressure analysis. These events cluster around the nine disposal wells (Fig. 7). A monitoring polygon was delineated to encompass both the seismic events (Fig. 7a) and disposal wells (Fig. 7b). Subsequently, the model was divided into two sectors: the induced seismicity sector and the non-induced seismicity sector (Fig. 8). This configuration serves two purposes: it enables sector-based pressure analysis within the seismicity zone, and it supports adaptive grid refinement during reservoir simulation by maintaining finer resolution in the induced seismicity sector while using coarser cells in the non-induced seismicity sector.

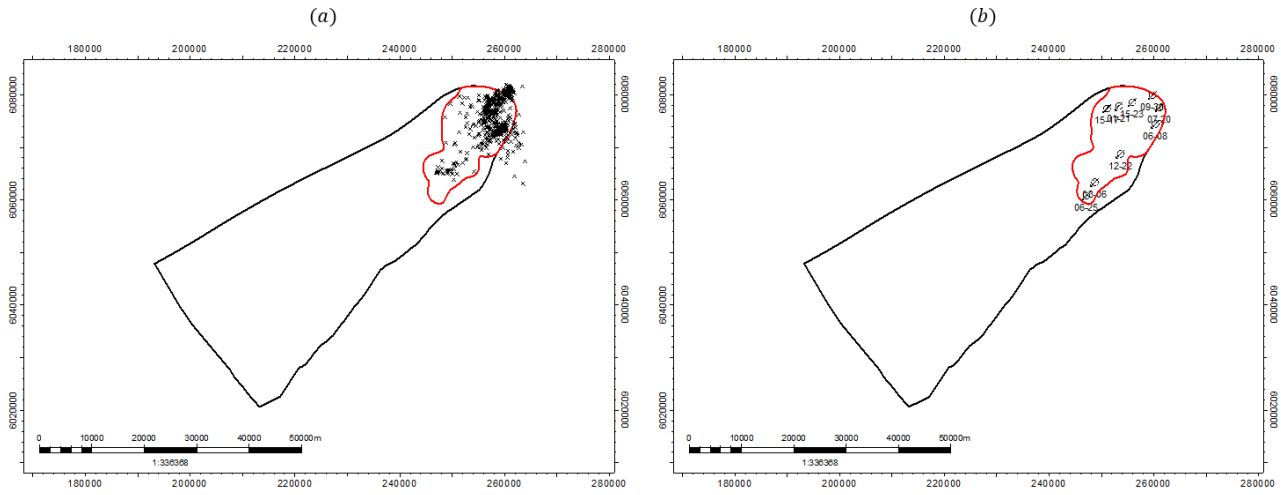


Figure 7. (a) Induced seismicity polygon (red) with induced seismicity events. (b) Induced seismicity polygon (red) with water disposal injectors.

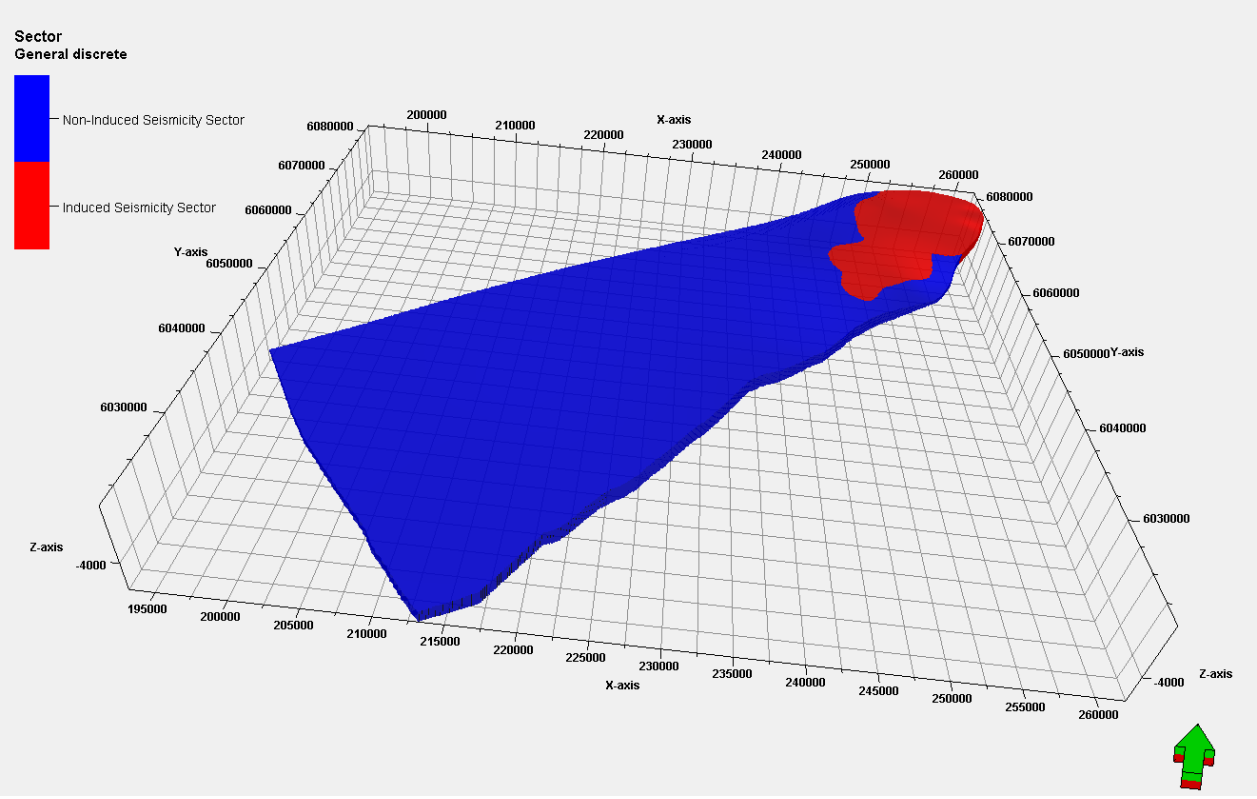


Figure 8. Geometrical model of induced seismicity sector.

Induced-Seismicity-Driven Pressure Buildup Analysis

Pressure models were built spanning April 2015 to April 2018 using bottom-hole pressure (BHP) fall-off tests from five wells: 06-08 (January 2016), well 07-20 (April 2015 and July 2016), well 15-23 (October 2017), well 09-30 (December 2017), and well 01-21 (April 2018). Figure 9 shows the 3D pressure distribution in the induced seismicity sector in April 2015 and April 2018, revealing pressure increase over time. Average pressure was calculated for the induced seismicity sector from each 3D model. The results show pressure increased during this period, tracking the rise in injection rates (Fig. 10). Notably, average pressure in the induced seismicity sector increased by approximately 10% between April 2015 and April 2018 following the onset of water injection. These tests document the relationship between disposal activities and pressure buildup in the region.

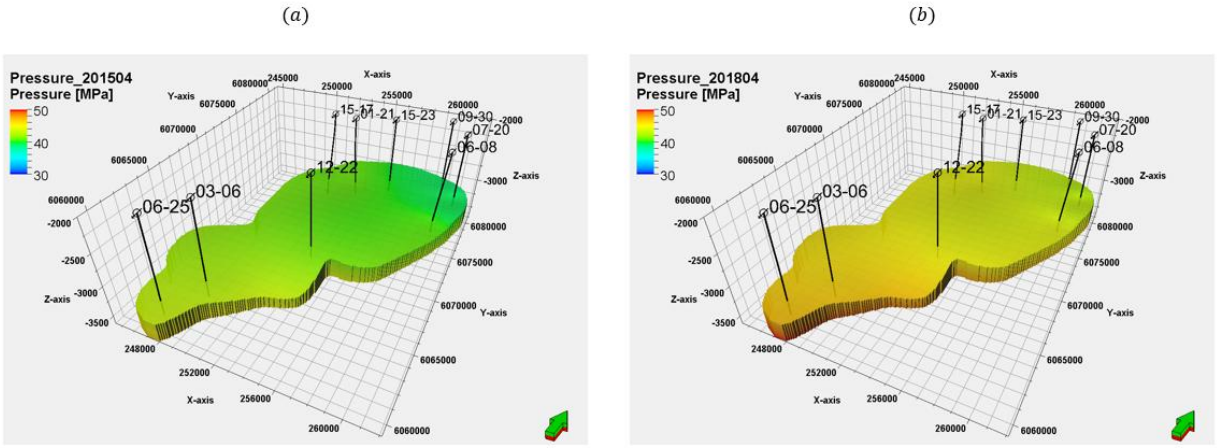


Figure 9. (a) Pressure model in April 2015. (b) Pressure model in April 2018.

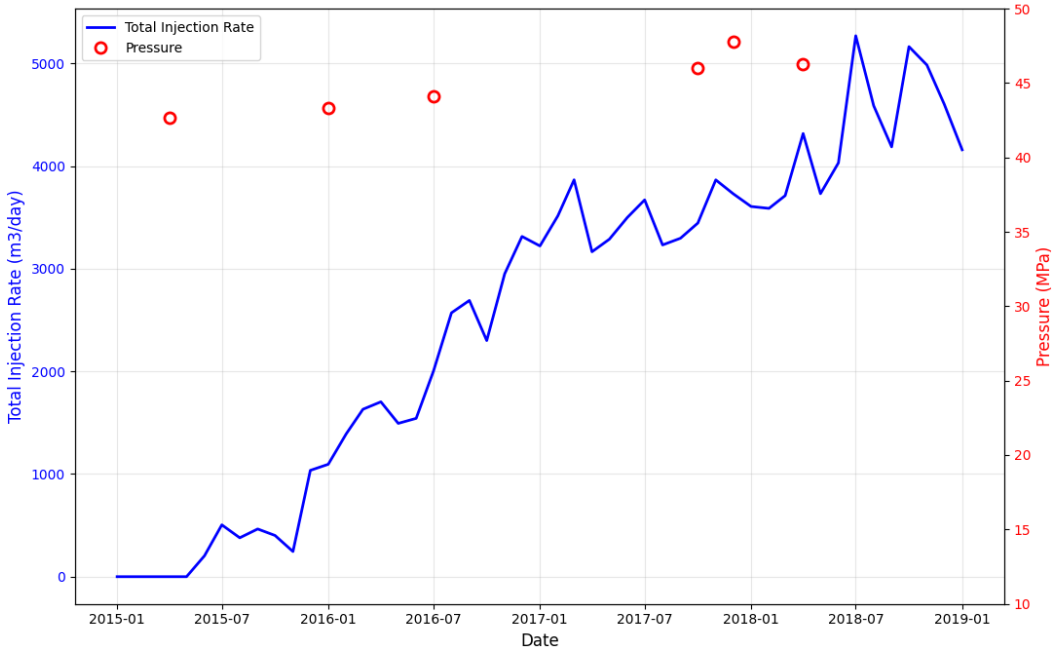


Figure 10. Relationship between total injection rate, average pressure in the induced seismicity sector and date.

Induced-Seismicity-Driven Simulation Model Upscaling and Local Grid Refinement

For reservoir simulation, the geological model was upscaled from 100 m × 100 m × 2 m to 500 m × 500 m × 4 m (Fig. 11a). However, a finer 100 m × 100 m × 2 m grid was used in the induced seismicity sector using local grid refinement (Fig. 11b). This maintains resolution where needed most to capture flow and pressure dynamics accurately. Detailed injection-pressure relationships and flow regime characterization will be assessed during the simulation phase.

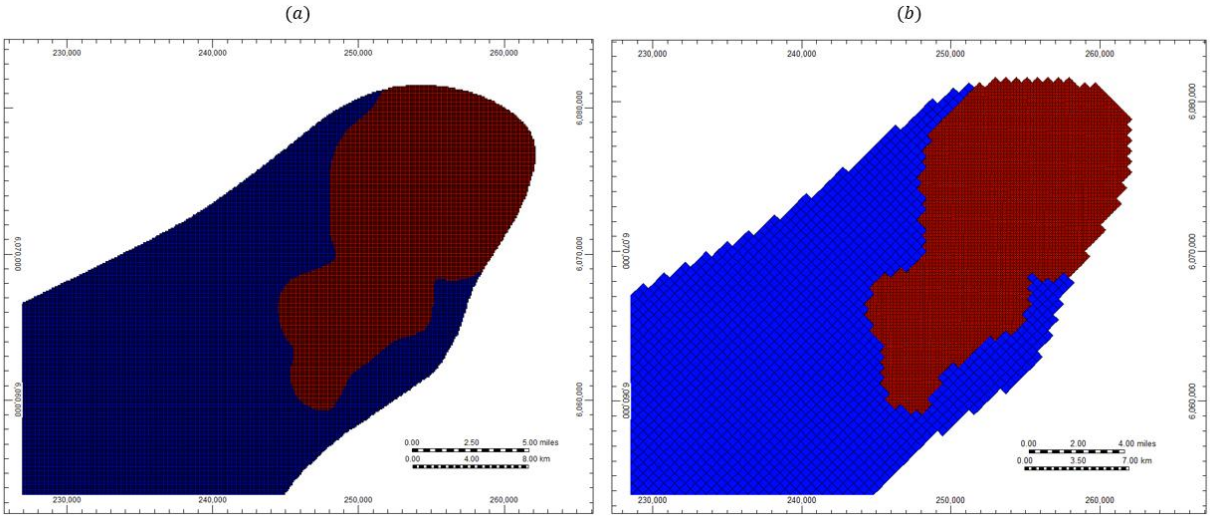


Figure 11. (a) Grid structure of geological model. (b) Grid structure of simulation model.

Conclusion

Geological modeling at the Alberta Energy Regulator of the subsurface in an area of known induced seismicity is providing important insight to the relationships between geology, disposal operations, and changes in seismicity over time. Although the project is in a preliminary state and more work is anticipated, a simulation-ready framework has been prepared. Key findings include:

1. Sector modeling of the Gold Creek seismic cluster distribution has allowed for focused pressure analysis. The delineated zone reflects seismicity through October 2025; continued pressure diffusion may expand this footprint by activating previously unaffected faults.
2. Induced-seismicity-driven pressure analysis: Reservoir pressure measurements show pressure buildup matching injection rate increases, linking Steep Creek disposal operations to the seismic activity.
3. Induced-seismicity-driven grid refinement: Local grid refinement maintains fine resolution in the Gold Creek seismic cluster area and coarse cells elsewhere, concentrating computational resources where seismicity indicates active processes.

References

[1] Reyes Canales, M.., Bui, H., Hauck, T.E., Yusifbayov, J. and Goerzen, C.D. (2025): Assessment of the Gold Creek and Kakwa seismic clusters in relation to disposal activities in the Leduc formation; Alberta Energy Regulator / Alberta Geological Survey, AER/AGS Presentation 2025-006.
[2] Barrett, K., & Rohr, K. (2014). The role of differential chemical compaction in the formation of the Gold Creek Collapse Structure, West Central Alberta. *Bulletin of Canadian Petroleum Geology*, *62*(3), 132-156.
[3] S&P Global. (2025). AccuMap. *S&P Global*.
[4] Alberta Geological Survey. (2025): Alberta Geological Survey earthquake dashboard. Retrieved from https://ags-aer.shinyapps.io/Seismicity_waveform_app/
[5] Townend, J., & Zoback, M. D. (2000). How faulting keeps the crust strong. Geology, 28(5), 399-402.
[6] Rubinstein, J. L., & Mahani, A. B. (2015). Myths and facts on wastewater injection, hydraulic fracturing, enhanced oil recovery, and induced seismicity. *Seismological Research Letters*, *86*(4), 1060-1067.
[7] Bachmann, C. E., Wiemer, S., Goertz-Allmann, B. P., & Woessner, J. (2012). Influence of pore-pressure on the event-size distribution of induced earthquakes. Geophysical Research Letters, 39(9).
[8] Stokes, S. M., Ge, S., Brown, M. R., Menezes, E. A., Sheehan, A. F., & Tiampo, K. F. (2023). Pore pressure diffusion and onset of induced seismicity. Journal of Geophysical Research: Solid Earth, 128(3), e2022JB026012.
[9] Chen, Qiang, and Amos Nur. "Pore fluid pressure effects in anisotropic rocks: mechanisms of induced seismicity and weak faults." Pure and Applied Geophysics 139, no. 3 (1992): 463-479.
[10] Zhai, G., Shirzaei, M., Manga, M., & Chen, X. (2019). Pore-pressure diffusion, enhanced by poroelastic stresses, controls induced seismicity in Oklahoma. Proceedings of the National Academy of Sciences, 116(33), 16228-16233.
[11] Xu, J., Chen, Z., & Li, R. (2014). 3D Geological modeling and uncertainty analysis of pilot pad in the Long Lake field with lean zone and shale layer. *GeoConvention*.
[12] Amthor, J. E., Mountjoy, E. W., & Machel, H. G. (1994). Regional-scale porosity and permeability variations in Upper Devonian Leduc buildups: implications for reservoir development and prediction in carbonates. *AAPG bulletin*, *78*(10), 1541-1558.